

A TECHNIQUE FOR GAIN ENHANCEMENT OF A WIDE-SLOT ANTENNA USING A BANDPASS FREQUENCY SELECTIVE SURFACE AS SUPERSTRATE

Ayan Chatterjee¹, Susanta Kumar Parui²

^{1,2} Dept. of Electronics & Tele-Comm. Engineering, Indian Institute of Engineering Science & Technology, Shibpur, Howrah, West Bengal, (India)

ABSTRACT

This paper presents a technique for gain enhancement of a wide band antenna using a low profile, bandpass frequency selective surface (FSS) as superstrate. The cascaded FSS structure with non-resonant unit cells in each layer allows in-phase transmission of waves radiated from the antenna over a frequency range of 5-8 GHz. The structure allows a gain enhancement of 2-4dBi in the range of 5.5-7.5 GHz and less for rest of frequencies in the band of operation. The FSS provides a very low insertion loss between the two transmission poles along with a linearly decreasing transmission phase over the band. The composite structure shows an impedance bandwidth of 62% with an average gain of 7dBi over 5-8 GHz with a peak gain of 10dBi.

Keywords: Gain, Frequency Selective Surface, Wide-Slot, Bandpass, Wideband

I. INTRODUCTION

Slot antennas offering wide band and ultra-wide band (UWB) properties are being widely used in ground penetrating radar (GPR), short range wireless communication [1]. In general, these antennas radiate in both directions orthogonal to the radiating plane whereas applications involving line-of-sight (LOS) communication and high signal to noise ratio (SNR) require semi-omnidirectional (wide-beam) radiation patterns [1-2]. Directional radiation from the antenna also provides enhanced gain in the broadside direction along with reduced side lobe levels (SLL) finding its application in the radar microwave and millimeter wave systems [4]. A broadside series-fed printed antenna array with a large slot in the ground plane was introduced [3] leading to enhancement in gain by about 2-3 dB over the whole band but a reasonable increase in the antenna size was required due to the array structure. Recently, Frequency Selective Surfaces (FSS) are being used in the form of substrates or superstrates [5-7] for the enhancement of antenna performances. Abbas Pirhadi et al. have investigated an electromagnetic bandgap (EBG) antenna [5] where a frequency selective surface (FSS) with square loop elements was used as a superstrate layer above the microstrip patch, leading to enhanced directivity. The use of FSS superstrates for dual-band directivity enhancement was introduced by Lee et al. [7] that comprise two FSS screens with about half wavelength spacing between them at a height of about half wavelength from the antenna which makes the overall height almost one wavelength and it is highly desirable to reduce for low profile applications. In most of such examples, the antenna parameters have been improved only over a narrow band or multiple frequency bands.

In this paper, a thin multilayered FSS structure has been used as a superstrate above a wide slot antenna to enhance its gain in one of the broadside directions over the entire frequency band of operation. The FSS, exhibiting band pass filtering property, consists of two thin dielectric sheets and three metallic layers

II. DESCRIPTION OF THE ANTENNA AND FSS

2.1 Design of the Slot Antenna

A microstrip line fed slot antenna design method was proposed by Jen-Yea Jan et al. [8]. Following this procedure, a slot antenna is designed in the frequency band of 5-8 GHz for the purpose of gain enhancement over the entire operating band. For exciting the first resonance of the antenna near 5.7 GHz, size of the square shaped slot has been chosen by the following equation:

$$\text{Slot length} = \frac{C_0}{2 \times f_r \times \sqrt{(\epsilon_r + 1)/2}} \quad (1)$$

Where C_0 is the speed of light in free space (3×10^8 m/s), f_r is the desired resonating frequency (5.7GHz) and ϵ_r ($\epsilon_r=4.4$) is the relative permittivity of the substrate which is FR4. The substrate thickness is $h_s = 1.6$ mm. The above equation (1) gives a slot length of 16mm as shown in the Fig. 2 below. To achieve the second resonance near 7.5 GHz, the slot has been rotated at an angle of 45° about y axis and for optimal matching, length of the microstrip feed line has been chosen to be 18.5mm.

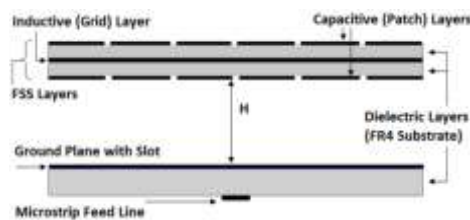


Fig. 1. Geometry of the FSS-Antenna Composite Structure (side view)

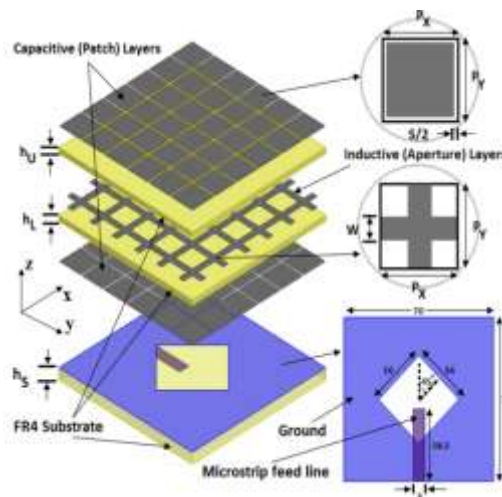


Fig. 2. A 3D View of Slot Antenna with FSS (All dimensions are in mm)

2.2 Design Principle of the FSS

The second order band pass response has been achieved by cascading three FSS layers of patch-aperture-patch type (as proposed in [9]) with FR4 as the dielectric material ($\epsilon_r=4.4$) in between them as shown in the Fig. 2. Unit cells of the patch and aperture type layers exhibiting capacitive and inductive properties respectively are also shown in the figure. They do so due to their non-resonant structure, where dimensions of the unit cells are much smaller than the wavelength corresponding to the resonating frequency of interest. Fig. 2 shows top view of each layer, where P_x and P_y are horizontal and vertical

periodicities of the unit cells same for both types of FSS screens and (P_x) is dimension of the patch in capacitive layer (s being the spacing between individual patches and $P_x = P_y = P$). Inductive wire grids have a grid width of w .

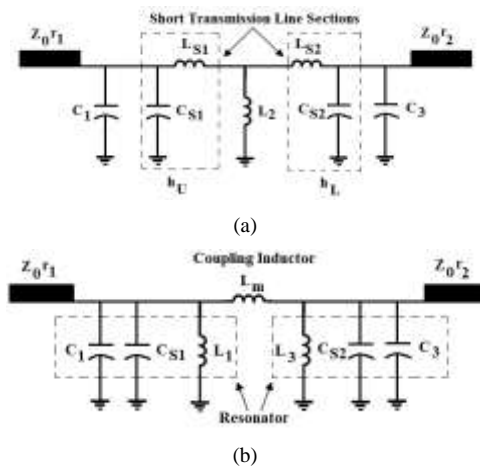


Fig. 3 (a) Simple equivalent circuit model of the cascaded FSS (b) Second order coupled resonator filter with π network (L_1, L_m and L_3) representation of T network (L_{S1}, L_2 and L_{S2})

A simple equivalent circuit of the FSS is given in Fig. 3(a). Being non-resonant in nature, the first and third patch type layers are modeled as parallel capacitors C_1 and C_3 , whereas the middle aperture type grid layer is modeled as a parallel inductor L_2 . Dielectric substrates separating the metallic FSS layers can be modeled as two short pieces of transmission lines of characteristic impedances $Z_0/\sqrt{\epsilon_{r1}}$ and $Z_0/\sqrt{\epsilon_{r2}}$ respectively, where ϵ_{r1} and ϵ_{r2} are dielectric constants of the two substrates and $Z_0 = 377\Omega$ is the free space impedance. The transmission line sections are represented here by their equivalent circuit model with a series inductor and a shunt capacitor. Half spaces on both ends of the cascaded FSS are modeled here as semi-infinite transmission lines with characteristic impedances of $Z_0 r_1$ and $Z_0 r_2$ respectively where r_1 and r_2 are the normalized source and load impedances and for free space $r_1 = r_2 = 1$. Second order nature of the filter is clearly visible in the circuit as shown in Fig. 3(b) where T network (consisting L_{S1}, L_2 and L_{S2}) of the circuit in Fig. 3(a) is converted into a π network (consisting L_1, L_m and L_3). The values of L_1, L_m and L_3 can be easily found with the values of L_{S1}, L_2 and L_{S2} .

As can be seen from the Fig.3(b), the circuit is a second order, coupled resonator band pass filter where two parallel LC resonators are coupled by a mutual inductance L_m and so the proposed FSS will act in a same manner as a second order band pass filter.

The FSS can be designed from the equivalent circuit model of Fig. 3(a). Prior to the design, the centre frequency of operation f_0 and the fractional bandwidth δ ($=BW/f_0$ corresponding to 3dB transmission bandwidth) are known for the filter and here these two parameters are decided based on operating frequency band (5-8 GHz) of the antenna. For the second order coupled resonator filter of Butterworth type response chosen, different parameters can be obtained from [10] and are given in Table 1.

Table 1. Different Parameters for Butterworth Filter Response

Filter Type	Normalized loaded quality factors		Normalized coupling coefficient	Normalized impedances	
	q_1	q_2	k_{12}	Source (r_1)	Load (r_2)
Butterworth	1.4142	1.4142	0.70711	1	1

From the desired values of f_0 and δ along with the parameters provided in Table 1, the value of inductor L_2 in the circuit of Fig. 3(a) can be found by the following equation [9]:

$$L_2 = \frac{Z_0}{(2\pi f_0)k_{12}} \times \frac{(k_{12}\delta)^2}{1-(k_{12}\delta)^2} \times \sqrt{\frac{r_1 r_2}{q_1 q_2}} \quad (2)$$

Using Telegrapher's model for TEM transmission lines, the inductors L_{S1} and L_{S2} representing the short transmission line sections of the circuit in the Fig. 3(a) can be calculated from the following equations:

$$L_{S1} = \mu_0 \mu_{r1} h_U(3) \quad \text{and} \quad L_{S2} = \mu_0 \mu_{r2} h_L(4)$$

The values of capacitors C_1 and C_3 representing the capacitive (patch) layers of FSS can also be obtained from the following equations [13]:

$$C_1 = \frac{q_1}{(2\pi f_0)Z_0 r_1 \delta} - \frac{\epsilon_0 \epsilon_{r1} h_U}{2} \quad (5)$$

$$C_3 = \frac{q_2}{(2\pi f_0)Z_0 r_2 \delta} - \frac{\epsilon_0 \epsilon_{r2} h_L}{2} \quad (6)$$

The above equations along with the substrate parameters are now used to determine the inductor (L_2) and capacitor (C_1, C_3) values of the Butterworth filter for desired response of FSS with centre frequency $f_0 = 6.5\text{GHz}$ and fractional bandwidth $\delta = 0.46$ (for 3dB transmission $BW=3\text{GHz}$). For available substrate thickness $h_U = h_L = 0.8\text{mm}$, the computed values are $C_1 = C_3 = 184.4\text{fF}$ and $L_2 = 1.1\text{nH}$. In the next step, dimensions of the unit cells of both the capacitive and inductive layers of the FSS are determined by the following equations [9].

$$C_1 = C_3 = C = \epsilon_0 \epsilon_{eff} \frac{2P}{\pi} \ln \left[\frac{1}{\sin \frac{\pi s}{2P}} \right] \quad (7)$$

$$L_2 = L = \mu_0 \mu_{eff} \frac{P}{2\pi} \ln \left(\frac{1}{\sin \frac{\pi w}{2P}} \right) \quad (8)$$

From equation (7), with $C = 184.4\text{fF}$, $s = 0.3\text{mm}$, ϵ_0 (free space permittivity) $= 8.85 \times 10^{-12} \text{ F/m}$ and ϵ_{eff} (effective permittivity) $= (\epsilon_r + 1)/2 = 2.7$, the unit cell dimension P is first obtained. The spacing between consecutive patches (s) is selected so to avoid fabrication errors, at the same time allowing good angular stability. Then with the value of P , $L = 1.1 \text{ nH}$, μ_0 (free space permeability) $= 4\pi \times 10^{-7} \text{ H/m}$ and μ_{eff} (effective permeability of the medium in which the inductive grids are located) $= (\mu_r + 1)/2 = 1$, width of the inductive wire grids is determined. With the initially available dimensions, after a few successive full wave EM simulations, optimal dimensions are obtained and are given in the Table 2 for the desired second order bandpass response. For EM simulations, HFSS is used.

Table 2 Optimal Dimensions of the Unit Cells of the FSS Layers

Parameter	$P_x = P_y = P$	w	s	$h_U = h_L$
Value	7mm	1.6mm	0.3mm	0.8mm

III. CHARACTERISTICS OF THE ANTENNA WITH FSS

3.1 Characteristics of the FSS

Transmission and reflection coefficients of the structure are then obtained using full wave EM simulation and are shown in Fig. 4(a) with the transmission phase (degree) variation with frequency in Fig. 4(b).

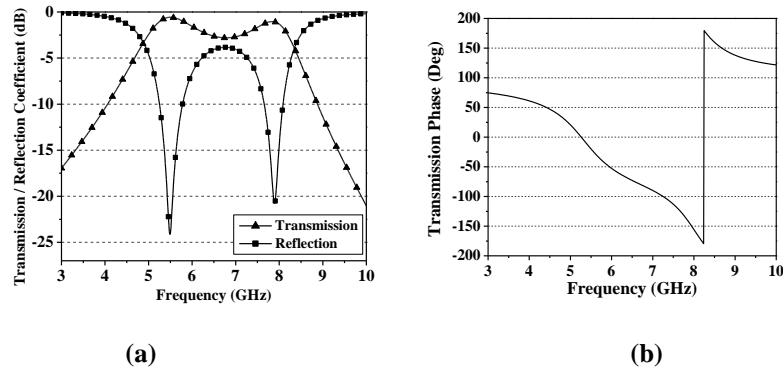


Fig. 4. Simulated (a) Transmission and Reflection Coefficient (b) Transmission Phase of the cascaded FSS structure
 As can be observed from Fig. 4(a), the FSS exhibits a pass band over 5-8 GHz with transmission level above -3 dB with two transmission poles. From the phase vs. frequency plot, it is clear that, the phase is zero at both the transmission poles and has nearly linear variation with frequency in between. The 3dB transmission as well as reflection bandwidth of the bandpass FSS is around 50% with respect to the centre frequency.

3.2 Characteristics of the Antenna with FSS

Simulated reflection coefficients (dB) of the antenna with and without FSS are shown in the Fig. 5 for different values of H. The height H is initially kept at $\lambda_0/2$ (λ_0 corresponding to the first resonating frequency) which is around 27mm and then slightly varied between 25mm and 31mm. The simulated impedance bandwidth of the antenna with FSS is 62% at H 27mm.

Simulated co and cross polar radiation patterns for the antenna with FSS are shown in the Fig. 6(a) and (b) for the frequency 6.32GHz (where maximum enhancement in gain is observed) for $\phi=90^\circ$ (E plane) and $\phi=0^\circ$ (H plane) planes respectively. Simulated results of gain variation for the antenna with FSS placed at different heights (H) are shown for comparison in the Fig. 7.

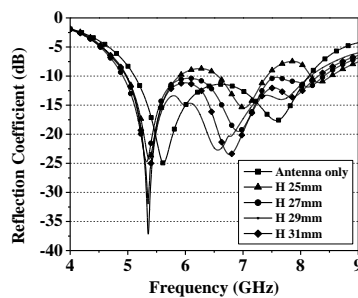
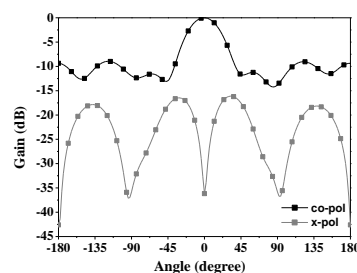


Fig. 5. Simulated reflection coefficient of the antenna with FSS superstrate at different height H for comparison



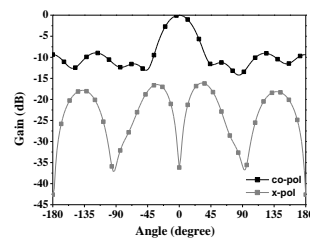
(a) E Plane ($\varphi=90^\circ$)(b) H Plane ($\varphi=0^\circ$)

Fig. 6. Simulated co and cross polar normalized radiation patterns for E and H planes of the antenna with FSS at 6.32GHz and H 27mm

Radiation from E plane offers difference of around 25dB between the co and cross polar components, whereas for the H plane, this difference is about 15dB. A gain of around 10dBi is noticed at 6.32GHz, whereas the gain is enhanced by 2-4dBi and maintained between 6-8 dBi over 5.5-7.5GHz and less for rest of the band.

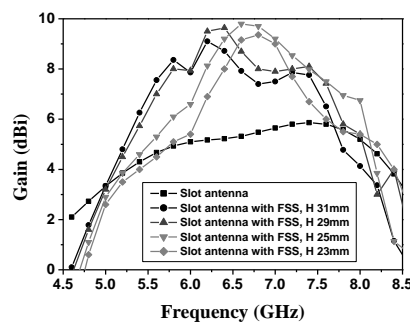


Fig. 7. Variation of gain of the slot antenna with FSS at different height H

IV. CONCLUSIONS

A wide slot antenna with a second order, band pass frequency selective surface has been studied. The structure is low profile because of non-resonant nature of the patch and grid type FSS layers. The proposed design achieves an impedance bandwidth of 62% and an average gain of 7 dBi over the operating frequency band of the antenna with a peak gain of 10dBi. The design also allows a variation of gap between the antenna and superstrate by around 4mm without significant degradation in its performance. Use of FSS as a shield allows the antenna to be used in close proximity of conductors without significant electromagnetic interference. The gap between FSS layers and the slot antenna is yet to be reduced for the purpose of further miniaturization.

REFERENCES

- [1]. S. Sharma, L. Shafai, N. Jacob, Investigation of Wide-Band Microstrip Slot Antenna. IEEE Trans. on Antennas and Prop., 2004, 52 (3), 865-872.
- [2]. Y. Sung, A Printed Wide-Slot Antenna with a Modified L-Shaped Microstrip Line for Wideband Applications. IEEE Trans. on Antennas and Prop., 2011, 59 (10), 3917-3922.

- [3]. R. Bayderkhani, H. Hassani, Wideband and Low Sidelobe Slot Antenna Fed by Series-Fed Printed Array. IEEE Trans. on Antennas and Prop., 2010, 58 (12),3898-3904.
- A. Nestic, Z. Micic, S. Jovanovic, I. Randonvic, Millimeter wave printed antenna array with high side lobe suppression. Proc. of IEEEAP-S International Symposium, 2006, 3051–3054.
- [4]. Pirhadi, H. Bahrami, J. Nasri, Wideband High Directive Aperture Coupled Microstrip Antenna Design by Using a FSS Superstrate Layer. IEEE Trans. on Antennas and Prop., 2012, 60 (4),2101-06.
- [5]. H-Y. Chen, Y. Tao, Performance Improvement of a U-Slot Patch Antenna Using a Dual-Band FSS With Modified Jerusalem Cross Elements. IEEE Trans. on Antennas and Prop., 2011, 59 (9), 3482-3486.
- [6]. Y.J. Lee, J. Yeo, R. Mittra, W.S. Park, Design of a FSS type superstrate for dual-band directivity enhancement of microstrip patch antennas. IEEE Antennas and Prop. Society Int. Symp., 2005, 3A, 2-5.
- [7]. J-Y. Jan, J-W.Su, Bandwidth Enhancement of a Printed Wide-Slot Antenna with a Rotated Slot. IEEE Trans. on Antennas and Prop., 2005, 53 (6), 2111-14.
- [8]. Al-Joumayly, Mudar; Behdad, Nader: A New Technique for Design of Low-Profile, Second-Order, Bandpass Frequency Selective Surfaces. IEEE Trans. on Antennas and Propag., 57 (2) 2009, 452-459.
- [9]. A. I. Zverev, Handbook of Filter Synthesis, 1967, Wiley, New York.